Bioorganic Chemistry 80 (2018) 693–705

Contents lists available at ScienceDirect

Bioorganic Chemistry

journal homepage: www.elsevier.com/locate/bioorg

Synthesis and DNase I inhibitory properties of some 5,6,7,8-tetrahydrobenzo[4,5]thieno[2,3-*d*]pyrimidines

Anelia Ts. Mavrova[a,*], Stefan Dimov[a], Denitsa Yancheva[b], Ana Kolarević[c], Budimir S. Ilić[d], Gordana Kocić[e], Andrija Šmelcerović[d,*]

[a] University of Chemical Technology and Metallurgy, 8 Kliment Ohridski Blvd., 1756 Sofia, Bulgaria
[b] Institute of Organic Chemistry with Centre of Phytochemistry, Bulgarian Academy of Science, Acad. G Bonchev Str., Build. 9, 1113 Sofia, Bulgaria
[c] Department of Pharmacy, Faculty of Medicine, University of Niš, 18000 Niš, Serbia
[d] Department of Chemistry, Faculty of Medicine, University of Niš, Bulevar Dr Zorana Đinđića 81, 18000 Niš, Serbia
[e] Institute of Biochemistry, Faculty of Medicine, University of Niš, Bulevar Dr Zorana Đinđića 81, 18000 Niš, Serbia

ARTICLE INFO

Keywords:
Thieno[2,3-*d*]pyrimidines
Synthesis
DNase I inhibition
R-Group analysis
Molecular docking
SAR analysis

ABSTRACT

A series of six novel and six known thieno[2,3-*d*]pyrimidin-4-amines **2–13** were synthesized, and further were used as a starting material for preparation of a small series of eight novel thieno[2,3-*d*]pyrimidin-4-phthalimides **14–21**. Eight compounds, five amine and three phthalimide derivatives, inhibited bovine pancreatic DNase I with an IC_{50} below 200 μM, being more effective than referent inhibitor crystal violet. Phthalimide derivatives **16**, **18** and **19** exhibited higher DNase I inhibitory activity compared to their amine precursors **7**, **10** and **11**. Compound **19**, as the most potent (IC_{50} = 106 ± 16 μM), offers a good starting point for a design of new DNase I inhibitors. The Pharma RQSAR model showed a significant enhancement of thieno[2,3-*d*]pyrimidines activity using aryl substituents at R1 position. The E-State RQSAR model clarified the most important structural fragments relevant for DNase I inhibition. Molecular docking and Site Finder module defined the thieno[2,3-*d*]pyrimidines interactions with the most important catalytic residues of DNase I, including Glu 39, His 134, Asp 168 and His 252. We also found that steric effects and increase of molecular volume play a vital role in DNase I inhibition.

1. Introduction

Deoxyribonuclease I (DNase I) is one of the best characterized endonuclease among mammals [1]. It is predominantly found in the exocrine pancreas [2]. DNase I catalyzes DNA hydrolysis by producing 3′-OH/5′-P ends and exerts its full activity in the presence of both Ca^{2+} and Mg^{2+} under neutral pH conditions [1]. On the other hand, DNase I inhibitors are compounds able to control or modify this process. Both DNase I and its inhibitors can be used as compounds for diagnosis, monitoring and therapy of various diseases [3–5]. It was shown that DNase I plays a fundamental role in apoptosis as possible mediator of internucleosomal DNA fragmentation [6–8]. This makes DNase I inhibitors an attractive potential target to design alternative strategies for the treatment of various disease conditions related with excessive apoptosis, including neurodegenerative diseases, ischemia-reperfusion injury, graft-versus-host disease and autoimmune disorders [8,9]. Recently, we reported ascorbic acid as a pioneer of substrate-based DNase I inhibitors [10].

The bioisosteric relation of thieno[2,3-*d*]pyrimidine-4-ones with quinolones, cytosine and uracil led to the generation of compounds with various biological properties, such as antibacterial [11,12], antiparasitic [13], analgesic [14], anti-inflammatory [15], anticancer [16], antioxidant [17], antiemetic [18], antiviral [19] and antihistaminic [20]. The structural biosterism with quinazoline analogue has been recently demonstrated to play an important role in the antibacterial and central nervous system (CNS) activity of thienopyrimidines [21,22]. Additionally, phthalimide derivatives exhibit multifaceted biological activity, such as anti-mycobacterium tuberculosis [23], anticonvulsant and neurotoxicity [24,25], analgesic and anti-inflammatory [26], as well as α-glucosidase inhibition [27] activities.

Taking into consideration the bioisosteric relationship between thieno[2,3-*d*]pyrimidines and the pyrimidine nucleosides, as well as their structural similarity (Fig. 1), in this study we synthesized a small library of 2-substituted 5,6,7,8-tetrahydrobenzo[4,5]thieno[2,3-*d*]pyrimidines and evaluated their inhibitory activity against bovine pancreatic DNase I *in vitro*. R-Group analysis and molecular docking are *in*

* Corresponding authors.
E-mail addresses: anmav@abv.bg (A. Ts. Mavrova), andrija.smelcerovic@medfak.ni.ac.rs (A. Šmelcerović).

https://doi.org/10.1016/j.bioorg.2018.07.009
Received 23 May 2018; Received in revised form 8 July 2018; Accepted 9 July 2018

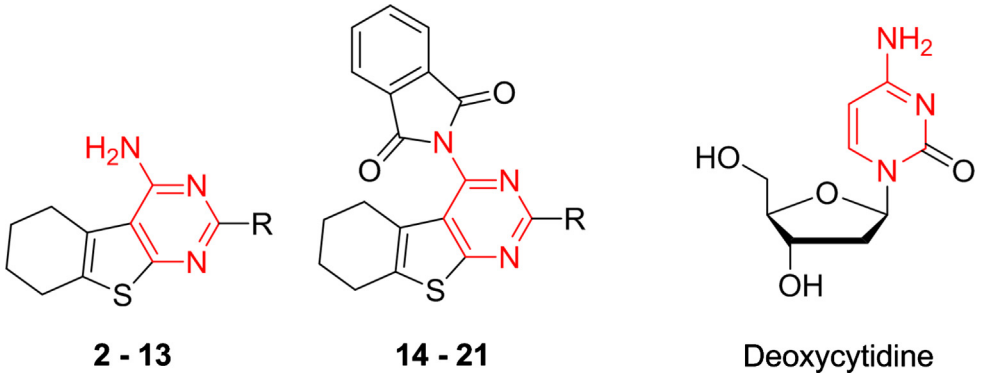

Fig. 1. Structural similarity of the synthesized thieno[2,3-*d*]pyrimidines and pyrimidine nucleoside deoxycytidine.

silico drug design methods used for better understanding of drug properties and target interaction that hypothesize the designing of novel drug candidates [28]. Having in mind that our studied molecules were built on a similar scaffold, by attaching different groups at one or more points on the thieno[2,3-*d*]pyrimidine, we wanted to examine DNase I inhibitory property of the thieno[2,3-*d*]pyrimidine-4-amines as a function of the groups at the various attachment points. In addition, we wanted to clarify DNase I inhibitory properties of thieno[2,3-*d*] pyrimidines at the molecular level using the Site Finder module and molecular docking studies. Finally, *in silico* study of the physico-chemical and toxicological properties of the studied compounds was performed.

2. Materials and methods

2.1. Synthesis

The synthesis of thieno[2,3-*d*]pyrimidine-4-amine derivatives containing phthalimide moiety is illustrated in Scheme 1.

The 2-aminothiophene-3-carbonitrile **1** was used as a starting material synthesized by Gewald reaction [29,30] which is a very often used reaction method for 2-aminothiophene synthesis. The 2-substituted thieno[2,3-*d*]pyrimidine-4-amines **2–13** were obtained by passing a stream of dry HCl gas through a dry dioxane solution of equimolar ratio of 2-aminothiophene **1** and alkyl or aryl nitriles for 6 h [31]. The bipharmacophoric derivatives **14–21** were synthesized by reaction of thieno[2,3-*d*]pyrimidine-4-amines **2–13** and phthalic anhydride in glacial acetic acid under reflux (method A) or in toluene/acetic anhydride/pyridine mixture (method B).

The chemical structure of the compounds was established by FT-IR, ^{1}H NMR and elemental analysis (^{1}H NMR and FT-IR data are provided in the Experimental part and some of the spectra in the Supplementary material – Figs. S1–S27).

Supplementary data associated with this article can be found, in the online version, at https://doi.org/10.1016/j.bioorg.2018.07.009.

Melting points (mp) were determined on an Electrothermal AZ 9000 3MK4 apparatus and were uncorrected. The thin layer chromatography (TLC, Rf values) was performed on F254 or silica gel plates F254

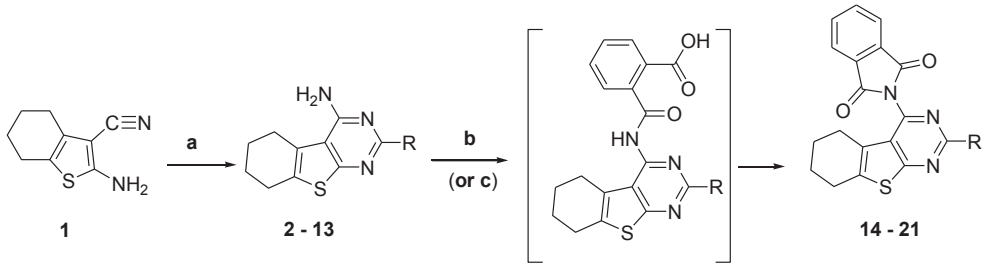

Comp.	R	Comp.	R	Comp.	R	Comp.	R
2		8		14		20	
3		9		15	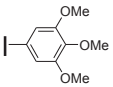	21	
4		10		16			
5		11	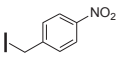	17			
6	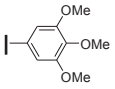	12		18			
7		13		19	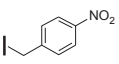		

Scheme 1. Synthesis of phthalimide derivatives of thieno[2,3-*d*]pyrimidine-4-amines: a) RCN, dry HCl gas, dioxane, 6 h; b) phthalic anhydride, acetic acid, reflux – method A; c) toluene, phthalic anhydride, acetic anhydride, pyridine – method B.

(Merck, 0.2 mm thick) and visualization was effected with ultraviolet light. IR spectra were recorded on a Bruker Equinox 55 spectrophotometer as potassium bromide discs. All ^{1}H NMR spectra were recorded on a Bruker Avance DRX 250 spectrometer (Bruker, Faelanden, Switzerland) operating at 250 MHz and a Bruker Avance DRX 600 spectrometer (Bruker, Faelanden, Switzerland) operating at 600 MHz. Chemical shifts were expressed relative to tetramethylsilane (TMS) and were reported as δ (*ppm*). The measurements were carried out at ambient temperature (300 K). The microanalyses for C, H, N and S were performed on PerkinElmer elemental analyzer. The UV–VIS absorption spectra were recorded on a spectrophotometer Hewlett Packard 8452A. The fluorescence spectra were taken on a Scinco FS-2 spectrofluorimeter.

*2.1.1. Synthesis of 2-aminothiophene-3-carbonitrile **1***

The synthesis of 2-aminothiophene-3-carbonitrile **1** was performed by cyclocondensation of cyclohexanone with malononitrile and sulfur in equimolar quantity with catalyst $HNEt_2$ as described by Sabnis et al. [30].

*2.1.2. General procedure for the synthesis of 5,6,7,8-tetrahydrobenzo[4,5]thieno[2,3-d]pyrimidin-4-amines **2–8, 10–13***

The corresponding 2-aminothiophene **1** (0.0094 mol), the appropriate cyano derivative RCN (0.0094 mol) and 20 mL of dioxane were mixed in a round flask whereat a stream of dry hydrogen chloride was passed through the solution for 6 h. The reaction mixture was allowed to stay for 12 h at room temperature. It was then poured into a beaker containing crushed ice and neutralized to pH ~ 8 using 10% (*v/v*) NH_4OH. The precipitate was filtered, washed many times with water and dried.

*2.1.2.1. 2-Benzyl-5,6,7,8-tetrahydrobenzo[4,5]thieno[2,3-d]pyrimidin-4-amine **(2)**.* The neutralisation resulted in resinous product, which was crystallized with pyridine. The formed precipitate was recrystallized from pyridine. Yield: 41%; Mp. 201–203 °C (lit. 193–195 °C [31]); IR (KBr): ν(cm^{-1}) 3382 (NH), 3293 (NH), 3187 (NH), 3023 (ArH), 2934 (CH), 2833 (CH), 1619 (NH), 718 (ArH); ^{1}H NMR (DMSO-d_6, δ): 1.78 (d, J = 2.7 Hz, 4H, $(CH_2)_2$), 2.71 (s, 2H, CH_2), 2.86 (s, 2H, CH_2), 3.94 (s, 2H, CH_2), 6.56–7.13 (bs, 2H, NH_2), 7.15–7.21 (m, 1H, ArH), 7.23–7.28 (m, 4H, ArH); Analysis: Calc. for $C_{17}H_{17}N_3S$: C, 69.12; H, 5.80; N, 14.22; S, 10.85; Found: C, 69.09; H, 5.79; N, 14.22; S, 10.90.

*2.1.2.2. Ethyl 2-(4-amino-5,6,7,8-tetrahydrobenzo[4,5]thieno[2,3-d]pyrimidin-2-yl)acetate **(3)**.* The neutralisation led to resinous product, which was crystallized with EtOAc. The formed precipitate was recrystallized from EtOAc. Yield: 52%; Mp. 170–172 °C (lit. 170–171 °C [31]); IR (KBr): ν(cm^{-1}) 3460 (NH), 3314 (NH), 3150 (NH), 2993 (CH), 2973 (CH), 2853 (CH), 1719 (C═O), 1650 (NH), 1196 (C—O); ^{1}H NMR (DMSO-d_6, δ): 1.17 (t, J = 7.1 Hz, 3H, CH_3), 1.79 (s, 4H, $(CH_2)_2$), 2.73 (s, 2H, CH_2), 2.88 (d, J = 1.8 Hz, 2H, CH_2), 3.67 (s, 2H, CH_2), 4.08 (q, J = 7.1 Hz, 2H, CH_2), 7.04–7.26 (bs, 2H, NH_2); Analysis: Calc. for $C_{14}H_{17}N_3O_2S$: C, 57.71; H, 5.88; N, 14.42; O, 10.98; S, 11.00; Found: C, 57.66; H, 5.85; N, 14.44; O, 10.97; S, 11.02.

*2.1.2.3. 2-(Pyridin-3-yl)-5,6,7,8-tetrahydrobenzo[4,5]thieno[2,3-d]pyrimidin-4-amine **(4)**.* The residue was recrystallized with dioxane and then it was isolated by preparational chomatography in a system of solvents EtOAc/Chloroform = 5:1. Yield: 30%; Mp. 286–288 °C (lit. 206–208 °C [31]); IR (KBr): ν(cm^{-1}) 3298 (NH), 3170 (NH), 3075 (ArH), 3008 (ArH), 2935 (CH), 1646 (NH); ^{1}H NMR (DMSO-d_6, δ): 1.80 (ddd, J = 16.6, 9.2, 4.9 Hz, 4H, $(CH_2)_2$), 2.77 (t, J = 6.0 Hz, 2H, CH_2), 2.91 (t, J = 6.0 Hz, 2H, CH_2), 7.55 (dd, J = 8.0, 4.8 Hz, 1H, ArH), 8.40–8.47 (m, 1H, ArH), 8.72 (dd, J = 4.7, 1.4 Hz, 1H, ArH), 9.23 (d, J = 1.9 Hz, 1H, ArH), 12.73 (s, 1H, NH, exchange with D_2O); Analysis: Calc. for $C_{15}H_{14}N_4S$: C, 63.80; H, 5.00; N, 19.84; S, 11.36; Found: C, 63.84; H, 4.07; N, 19.79; S, 11.32.

*2.1.2.4. 2-(Morpholinomethyl)-5,6,7,8-tetrahydrobenzo[4,5]thieno[2,3-d]pyrimidin-4-amine **(5)**.* The formed pyrimidine was recrystallized from MeOH. Yield: 40%; Mp. 224–225 °C; IR (KBr): ν(cm^{-1}) 3445 (NH), 3309 (NH), 3241 (NH), 3091 (ArH), 3010 (ArH), 2945 (CH), 2884 (CH), 2847 (CH), 1654 (NH), 1114 (C—O); ^{1}H NMR (DMSO-d_6, δ): 1.84 (t, J = 2.8 Hz, 4H, $(CH_2)_2$), 2.50 (m, 4H, CH_2–O–CH_2), 2.88 (d, J = 2.1 Hz, 2H, CH_2), 3.00 (d, J = 2.0 Hz, 2H, CH_2), 3.52 – 3.60 (m, 4H, CH_2–N–CH_2), 3.73 (s, 2H, CH_2). ^{1}H NMR ($CDCl_3$, δ) 1.71–1.82 (m, 4H, $(CH_2)_2$), 2.45 (s, 4H, CH_2–O–CH_2), 2.72 (t, J = 6.0 Hz, 2H, CH_2), 2.85 (t, J = 6.1 Hz, 2H, CH_2), 3.41 (s, 2H, CH_2), 3.52–3.61 (m, 4H, CH_2–N–CH_2), 12.03 (s, 1H, NH, exchange with D_2O); Analysis: Calc. for $C_{15}H_{20}N_4OS$: C, 59.18; H, 6.62; N, 18.41; O, 5.26; S, 10.53; Found: C, 59.20; H, 6.62; N, 18.40; O, 5.27; S, 10.53.

*2.1.2.5. 2-(3,4,5-Trimethoxyphenyl)-5,6,7,8-tetrahydrobenzo[4,5]thieno[2,3-d]pyrimidin-4-amine **(6)**.* The formed precipitate was recrystallized from pyridine and washed with MeOH. Yield: 43%; Mp. 214–215 °C; IR (KBr): ν(cm^{-1}) 3542 (NH), 3397 (NH), 2986 (CH), 2930 (CH), 2834 (CH), 1645 (NH), 1106 (C—O); ^{1}H NMR (DMSO-d_6, δ): 1.82 (s, 4H, $(CH_2)_2$), 2.76 (s, 2H, CH_2), 2.93 (s, 2H, CH_2), 3.72 (s, 3H, OCH_3), 3.87 (s, 6H, $2OCH_3$), 6.86 (s, 2H, NH_2), 7.69 (s, 2H, ArH); Analysis: Calc. for $C_{19}H_{21}N_3O_3S$: C, 61.44; H, 5.70; N, 11.31; O, 12.92; S, 8.63; Found: C, 61.41; H, 5.73; N, 11.28; O, 12.90; S, 8.63.

*2.1.2.6. 2-(Pyridin-2-yl)-5,6,7,8-tetrahydrobenzo[4,5]thieno[2,3-d]pyrimidin-4-amine **(7)**.* The compound was recrystallized with system of solvents Benzene/MeOH = 1:1. Yield: 45%; Mp. 264–266 °C (lit. 249–251 °C [31]); IR (KBr): ν(cm^{-1}) 3487 (NH), 3270 (NH), 3138 (NH), 2925 (CH), 2835 (CH), 1635 (NH), 740 (Ar-R); ^{1}H NMR (DMSO-d_6, δ): 1.83 (s, 4H, $(CH_2)_2$), 2.79 (s, 2H, CH_2), 2.95 (s, 2H, CH_2), 6.99 (bs, 2H, NH_2), 7.45 (dd, J = 6.7, 4.8 Hz, 1H, ArH), 7.91 (td, J = 7.8, 1.7 Hz, 1H, ArH), 8.32 (d, J = 7.9 Hz, 1H, ArH), 8.67 (d, J = 4.2 Hz, 1H, ArH); Analysis: Calc. for $C_{15}H_{14}N_4S$: C, 63.80; H, 5.00; N, 19.84; S, 11.36; Found: C, 63.81; H, 5.02; N, 19.81; S, 11.39.

*2.1.2.7. 2-(2-Chloroethyl)-5,6,7,8-tetrahydrobenzo[4,5]thieno[2,3-d]pyrimidin-4-amine **(8)**.* The formed precipitate was recrystallized from MeOH to give 20% yield as a white crystals. Mp. 170–172 °C; IR (KBr): ν(cm^{-1}) 3488 (NH), 3301 (NH), 3112 (NH), 2938 (CH_3), 2840 (CH_2), 1644 (NH); ^{1}H NMR (DMSO-d_6, δ): 1.78 (d, J = 2.8 Hz, 4H, $(CH_2)_2$), 2.71 (s, 2H, CH_2), 2.86 (s, 2H, CH_2), 3.07 (t, J = 6.6 Hz, 2H, CH_2), 4.01 (t, J = 6.6 Hz, 2H, CH_2), 6.75 (bs, 2H, NH_2); Analysis: Calc. for $C_{12}H_{14}ClN_3S$: C, 53.82; H, 5.27; Cl, 13.24; N, 15.69; S, 11.97; Found: C, 53.86; H, 5.31; Cl, 13.24; N, 15.67; S, 11.90.

*2.1.2.8. 2-Ethyl-5,6,7,8-tetrahydrobenzo[4,5]thieno[2,3-d]pyrimidin-4-amine **(10)**.* The formed precipitate was recrystallized from MeOH. Yield: 37%; Mp. 174–176 °C; IR (KBr): ν(cm^{-1}) 3491 (NH), 3446 (NH), 3303 (NH), 3133 (NH), 2943 (CH_3), 2841 (CH_2), 1639 (NH); ^{1}H NMR (DMSO-d_6, δ): 1.20 (t, J = 7.6 Hz, 3H, CH_3), 1.79 (t, J = 2.6 Hz, 4H, $(CH_2)_2$), 2.63 (q, J = 7.6 Hz, 2H, CH_2), 2.71 (d, J = 2.0 Hz, 2H, CH_2), 2.87 (d, J = 1.9 Hz, 2H, CH_2), 6.71 (bs, 2H, NH_2); Analysis: Calc. for $C_{12}H_{15}N_3S$: C, 61.77; H, 6.48; N, 18.01; S, 13.74; Found: C, 61.79; H, 6.51; N, 18.01; S, 13.74.

*2.1.2.9. 2-(4-Nitrobenzyl)-5,6,7,8-tetrahydrobenzo[4,5]thieno[2,3-d]pyrimidin-4-amine **(11)**.* The mixture was left for 12 h after neutralization to crystallize. The product was recrystallized with system of solvents DMSO/MeOH = 5:1. Yield: 51%; Mp. 248–250 °C (lit. 320–322 °C [31]); IR (KBr): ν(cm^{-1}) 3491 (NH), 3300 (NH), 3102 (NH), 2942 (CH_2), 2835 (CH_2), 1642 (NH), 1517 (NO_2), 1343 (NO_2), 723 cm^{-1} (ArH); ^{1}H NMR (DMSO-d_6, δ): 1.78 (s, 4H, $(CH_2)_2$), 2.71 (s, 2H, CH_2), 2.86 (s, 2H, CH_2), 4.11 (s, 2H, CH_2), 6.83 (bs, 2H, NH_2), 7.53 (d, J = 8.8 Hz, 2H, ArH), 8.11–8.17 (m, 2H, ArH); Analysis: Calc. for $C_{17}H_{16}N_4O_2S$: C, 59.98; H, 4.74; N, 16.46; O, 9.40; S, 9.42; Found: C, 59.93; H, 4.75; N, 16.46; O, 9.43; S, 9.41.

*2.1.2.10. 2-(3-Chlorobenzyl)-5,6,7,8-tetrahydrobenzo[4,5]thieno[2,3-d] pyrimidin-4-amine (**12**).* The mixture was titrated up to alkaline pH and left for a night. In result the resinous product crystallized. The product was recrystallized with pyridine and washed with MeOH. Yield: 48%; Mp. 210–212 °C; IR (KBr): ν(cm^{-1}) 3491 (NH), 3306 (NH), 3094 (ArH), 2928 (CH_2), 2834 (CH_2), 1646 (NH), 783, 740, 682 (ArH); ^{1}H NMR (DMSO-d_6, δ): 1.78 (s, 4H, $(CH_2)_2$), 2.71 (s, 2H, CH_2), 2.87 (s, 2H, CH_2), 3.96 (s, 2H, CH_2), 6.80 (bs, 2H, NH_2), 7.22 (d, J = 7.5 Hz, 1H, ArH), 7.24–7.27 (m, 1H, ArH), 7.31 (dd, J = 10.3, 5.0 Hz, 2H, ArH); Analysis: Calc. for $C_{17}H_{16}ClN_3S$: C, 61.90; H, 4.89; Cl, 10.75; N, 12.74; S, 9.72; Found: C, 61.90; H, 4.88; Cl, 10.75; N, 12.72; S, 9.71.

*2.1.2.11. 2-(3-(Trifluoromethyl)phenyl)-5,6,7,8-tetrahydrobenzo[4,5] thieno[2,3-d]pyrimidin-4-amine (**13**).* The mixture titrated up to alkaline pH and left for a night. In result the resinous product crystallized. The product was recrystallized with acetic acid. Yield: 57%; Mp. 244–246 °C; IR (KBr): ν(cm^{-1}) 3476 (NH), 3279 (NH), 3162 (NH), 2945 (CH_2), 2846 (CH_2), 1646 (ArH), 1117 (C − F), 691 (ArH); ^{1}H NMR (DMSO-d_6, δ): 1.82 (s, 4H, $(CH_2)_2$), 2.78 (s, 2H, CH_2), 2.94 (s, 2H, CH_2), 7.02 (bs, 2H, NH_2), 7.72 (t, J = 7.8 Hz, 1H, ArH), 7.83 (d, J = 7.7 Hz, 1H, ArH), 8.60–8.65 (m, 2H, ArH); Analysis: Calc. for $C_{17}H_{14}F_3N_3S$: C, 58.44; H, 4.04; F, 16.31; N, 12.03; S, 9.18; Found: C, 58.45; H, 4.07; F, 16.33; N, 12.01; S, 9.10.

*2.1.3. Synthesis of 5,6,7,8-tetrahydrobenzo[4,5]thieno[2,3-d]pyrimidin-4-amine **9***

A steam of dry hydrogen chloride gas was passed through the solution of compound **1** (0.01 mol) and 30 mL dry acetonitrile for 6 h. The reaction mixture was allowed to stay for 12 h at room temperature. Then the mixture was poured into a beaker containing crushed ice and neutralized to pH ~ 8 using 10% NH_2OH. The product was recrystallized with system of solvents benzene/MeOH = 1:1. Yield: 81%; Mp. 233–234 °C (lit. 224–225 °C [31]); IR (KBr): ν(cm^{-1}) 3446 (NH), 3303 (NH), 3133 (NH), 2931 (CH_3), 2951 (CH_2), 2907 (CH_2), 1639 (NH); ^{1}H NMR (DMSO-d_6, δ): 1.79 (t, J = 2.5 Hz, 4H, $(CH_2)_2$), 2.36 (s, 3H, CH_3), 2.71 (d, J = 1.9 Hz, 2H, CH_2), 2.86 (d, J = 1.9 Hz, 2H, CH_2), 6.70 (bs, 2H, NH_2); Analysis: Calc. for $C_{11}H_{13}N_3S$: C, 60.24; H, 5.97; N, 19.16; S, 14.62; Found: C, 60.24; H, 5.99; N, 19.16; S, 14.62.

*2.1.4. General procedure for the synthesis of 5,6,7,8-tetrahydrobenzo[4,5] thieno[2,3-d]pyrimidin-4-phthalimides **14–21***

Method A. The corresponding thieno[2,3-*d*]pyrimidin-4-amine **2–13** (0.0017 mol) and 0.28 g phthalic anhydride (0.0019 mol) in 25 mL glacial acetic acid were mixed in a round-bottom flask. The solution was refluxed and the reaction was monitored by TLC. After the reaction was completed the mixture was poured into water and neutralized with 10% (*v/v*) NH_4OH to pH ~ 7. The precipitate formed was filtered and washed thoroughly with water.

Method B. To a solution of 0.0012 mol phthalic anhydride in toluene, 0.001 mol of the corresponding thieno[2,3-*d*]pyrimidin-4-amine was added in and the reaction mixture was refluxed for 5 h. The reaction solution was cooled to room temperature, 0.002 mol of acetic anhydride and 0.008 mol of pyridine were added and the refluxing was continued for 1 to 3 h. The solution was cooled in an ice bath, water was added to the reaction mixture, the organic layer was separated and after drying concentrated under reduced pressure, whereby the isoindoldiones crystallized.

*2.1.4.1. 2-(2-Benzyl-5,6,7,8-tetrahydrobenzo[4,5]thieno[2,3-d]pyrimidin-4-yl)isoindoline-1,3-dione (**14**).* Method A: The reaction mixture was refluxed for 40 h. The product crystallized after cooling. The compound was purified by double recrystallization from acetic acid. Yield: 12%; Mp. = 222–225 °C; IR (KBr): ν(cm^{-1}) 3082 (ArH), 3059 (ArH), 3028 (ArH), 2949 (CH), 1784 (C═O), 1725 (C═O), 721 (ArH); ^{1}H NMR ($CDCl_3$, δ): 1.72–1.92 (m, 4H, $(CH_2)_2$), 2.56 (t, J = 6.2 Hz, 2H, CH_2), 2.88 (t, J = 6.1 Hz, 2H, CH_2), 4.44 (s, 2H, CH_2), 7.23 (t, J = 7.4 Hz, 1H, ArH), 7.31 (t, J = 7.6 Hz, 2H, ArH), 7.42 (d, J = 7.3 Hz, 2H, ArH), 7.88 (dd, J = 5.4, 3.1 Hz, 2H, ArH), 8.03 (dd, J = 5.5, 3.0 Hz, 2H, ArH); Analysis: Calc. for $C_{25}H_{19}N_3O_2S$: C, 70.57; H, 4.50; N, 9.88; O, 7.52; S, 7.54; Found: C, 70.53; H, 4.49; N, 9.83; O, 7.52; S, 7.53. Method B: Yield: 63%.

*2.1.4.2. 2-(2-(3,4,5-Trimethoxyphenyl)-5,6,7,8-tetrahydrobenzo[4,5] thieno[2,3-d]pyrimidin-4-yl) isoindoline-1,3-dione (**15**).* Method A: The reaction mixture was refluxed for 28 h. After cooling, the compound crystallized as white crystals. The product was purified by double recrystallization from acetic acid. Yield: 21%; Mp. = 269–270 °C; IR (KBr): ν(cm^{-1}) 3003 (ArH), 2965 (CH), 2935 (CH), 2835 (CH), 1788 (C═O), 1726 (C═O), 718 (ArH); ^{1}H NMR ($CDCl_3$): δ(ppm) = 1.75–1.96 (m, 4H, $(CH_2)_2$), 2.62 (dt, J = 27.0, 6.1 Hz, 2H, CH_2), 2.93 (dd, J = 12.4, 6.3 Hz, 2H, CH_2), 3.96 (dd, J = 28.8, 16.6 Hz, 9H, $3OCH_3$), 7.18, 7.83 (ds, 2H, ArH), 7.90 (ddd, J = 15.8, 5.4, 3.1 Hz, 2H, ArH), 8.06 (ddd, J = 20.2, 5.4, 3.1 Hz, 2H, ArH); Analysis: Calc. for $C_{27}H_{23}N_3O_5S$: C, 64.66; H, 4.62; N, 8.38; O, 15.95; S, 6.39; Found: C, 64.70; H, 4.64; N, 8.38; O, 15.96; S, 6.37; Method B: Yield: 51%.

*2.1.4.3. 2-(2-(Pyridin-2-yl)-5,6,7,8-tetrahydrobenzo[4,5]thieno[2,3-d] pyrimidin-4-yl)isoindoline-1,3-dione (**16**).* Method A: The reaction mixture was refluxed for 30 h. The product was purified by eluent system of Benzene/MeOH = 1:3. Yield: 15%; Mp. = 282–285 °C; IR (KBr): ν(cm^{-1}) 3066 (ArH), 2932 (CH), 2884 (CH), 2837 (CH), 1783 (C═O), 1721 (C═O), 721 (ArH); ^{1}H NMR (DMSO-d_6, δ): 1.71 (dd, J = 7.6, 4.0 Hz, 2H, CH_2), 1.82 (dd, J = 7.5, 3.9 Hz, 2H, CH_2), 2.55 (t, J = 6.0 Hz, 2H, CH_2), 2.96 (t, J = 6.1 Hz, 2H, CH_2), 7.56 (ddd, J = 7.5, 4.7, 1.1 Hz, 1H, ArH), 8.00 (td, J = 7.8, 1.8 Hz, 1H, ArH), 8.05 (dd, J = 5.4, 3.1 Hz, 2H, ArH), 8.14 (dd, J = 5.5, 3.0 Hz, 2H, ArH), 8.45 (dt, J = 8.0, 1.0 Hz, 1H, ArH), 8.76 (ddd, J = 4.7, 1.8, 0.9 Hz, 1H, ArH); Analysis: Calc. for $C_{23}H_{16}N_4O_2S$: C, 66.97; H, 3.91; N, 13.58; O, 7.76; S, 7.77; Found: C, 66.99; H, 3.92; N, 13.56; O, 7.76; S, 7.77; Method B: Yield: 44%.

*2.1.4.4. 2-(2-Methyl-5,6,7,8-tetrahydrobenzo[4,5]thieno[2,3-d] pyrimidin-4-yl)isoindoline-1,3-dione (**17**).* Method A: The reaction mixture was refluxed for 46 h. The product was isolated by hot filtration with MeOH, whereupon by cooling of the filtrate the pure product crystallized. Yield: 17%; Mp. = 201–202 °C; IR (KBr): ν(cm^{-1}) 2934 (CH), 2864 (CH), 1784 (C═O), 1722 (C═O), 718 (ArH); ^{1}H NMR (DMSO-d_6, δ): 1.67 (dt, J = 5.7, 4.6 Hz, 2H, CH_2), 1.78 (dt, J = 8.7, 4.7 Hz, 2H, CH_2), 2.45 (t, J = 6.1 Hz, 2H, CH_2), 2.75 (s, 3H, CH_3), 2.88 (t, J = 6.0 Hz, 2H, CH_2), 8.01 (dd, J = 5.5, 3.1 Hz, 2H, ArH), 8.09 (dd, J = 5.5, 3.0 Hz, 2H, ArH); Analysis: Calc. for $C_{19}H_{15}N_3O_2S$: C, 65.31; H, 4.33; N, 12.03; O, 9.16; S, 9.18; Found: C, 65.31; H, 4.35; N, 12.03; O, 9.18; S, 9.18; Method B: Yield: 65%.

*2.1.4.5. 2-(2-Ethyl-5,6,7,8-tetrahydrobenzo[4,5]thieno[2,3-d]pyrimidin-4-yl)isoindoline-1,3-dione (**18**).* Method A: The reaction mixture was refluxed for 34 h. The product was isolated by hot filtration with MeOH, then after crystallization the product was twice recrystallized from MeOH. Yield: 16%; Mp. = 156–157 °C; IR (KBr): ν(cm^{-1}) 3056 (ArH), 2940 (CH), 2871 (CH), 2839 (CH), 1786, 1764 (C═O), 1724 (C═O), 714 (ArH); ^{1}H NMR (DMSO-d_6, δ): 1.32 (t, J = 7.6 Hz, 3H, CH_3), 1.63–1.71 (m, 2H, CH_2), 1.75–1.82 (m, 2H, CH_2), 2.46 (t, J = 6.1 Hz, 2H, CH_2), 2.88 (t, J = 6.1 Hz, 2H, CH_2), 3.03 (q, J = 7.6 Hz, 2H, $\underline{CH_2}CH_3$), 8.02 (dd, J = 5.5, 3.1 Hz, 2H, ArH), 8.09 (dd, J = 5.5, 3.0 Hz, 2H, ArH); Analysis: Calc. for $C_{20}H_{17}N_3O_2S$: C, 66.10; H, 4.71; N, 11.56; O, 8.80; S, 8.82; Found: C, 66.09; H, 4.75; N, 11.50; O, 8.83; S, 8.83; Method B: Yield: 45%.

*2.1.4.6. 2-(2-(4-Nitrobenzyl)-5,6,7,8-tetrahydrobenzo[4,5]thieno[2,3-d] pyrimidin-4-yl)isoindoline-1,3-dione (**19**).* Method A: The reaction mixture was refluxed for 8 h. After the neutralization, the product was purified by TLC developed with EtOAc/*n*-Hex = 2:5. Yield: 12%;

Mp. = 223–225 °C; IR (KBr): $\nu(cm^{-1})$ 3082 (ArH), 3059 (ArH), 3028 (ArH), 2949 (CH), 1784 (C═O), 1725 (C═O), 721 (ArH); ^{1}H NMR (DMSO-d_6, δ): 1.66 (dd, J = 7.5, 3.9 Hz, 2H, CH_2), 1.75–1.81 (m, 2H, CH_2), 2.47 (t, J = 6.2 Hz, 2H, CH_2), 2.89 (t, J = 6.0 Hz, 2H, CH_2), 4.54 (s, 2H, CH_2), 7.61 (d, J = 8.8 Hz, 2H, ArH), 8.02 (dd, J = 5.5, 3.1 Hz, 2H, ArH), 8.09 (dd, J = 5.5, 3.0 Hz, 2H, ArH), 8.16–8.20 (m, 2H, ArH); Analysis: Calc. for $C_{25}H_{18}N_4O_4S$: C, 63.82; H, 3.86; N, 11.91; O, 13.60; S, 6.82; Found: C, 63.83; H, 3.90; N, 11.91; O, 13.62; S, 6.80; Method B: Yield: 54%.

2.1.4.7. 2-(2-(3-Chlorobenzyl)-5,6,7,8-tetrahydrobenzo[4,5]thieno[2,3-d]pyrimidin-4-yl)isoindoline-1,3-dione ***(20)***. Method A: The reaction mixture was refluxed for 30 h. After cooling the crystallized thienopyrimidine **12** was filtrated and the mixture neutralized. The residue was purified by recrystallization from acetic acid, giving the desired compound **20**. Yield: 10%; Mp. = 191–193 °C; IR (KBr): $\nu(cm^{-1})$ 3058 (ArH), 2931 (CH), 2856 (CH), 1787 (C═O), 1720 (C═O), 716 (ArH); ^{1}H NMR (DMSO-d_6, δ): 1.66 (dd, J = 7.4, 4.0 Hz, 2H, CH_2), 1.78 (dd, J = 7.5, 4.0 Hz, 2H, CH_2), 2.47 (t, J = 6.1 Hz, 2H, CH_2), 2.88 (t, J = 6.0 Hz, 2H, CH_2), 4.38 (s, 2H, CH_2), 7.27–7.31 (m, 2H, ArH), 7.32–7.36 (m, 1H, ArH), 7.39 (s, 1H, ArH), 8.01 (dd, J = 5.5, 3.1 Hz, 2H, ArH), 8.09 (dd, J = 5.5, 3.0 Hz, 2H, ArH); Analysis: Calc. for $C_{25}H_{18}ClN_3O_2S$: C, 65.28; H, 3.94; Cl, 7.71; N, 9.14; O, 6.96; S, 6.97; Found: C, 65.25; H, 3.98; Cl, 7.71; N, 9.19; O, 6.98; S, 6.96; Method B: Yield: 47%.

2.1.4.8. 2-(2-(3-(Trifluoromethyl)phenyl)-5,6,7,8-tetrahydrobenzo[4,5]thieno[2,3-d]pyrimidin-4-yl) isoindoline-1,3-dione ***(21)***. Method A: The reaction mixture was refluxed for 29 h and after cooling the desired imide product **21** crystallized. The residue was recrystallized from acetic acid. Yield: 35%; Mp. = 233–234 °C; IR (KBr): $\nu(cm^{-1})$ 3073 (ArH), 3026 (ArH), 2940 (CH), 2837 (CH), 1788 (C═O), 1718 (C═O), 724, 660 (ArH); ^{1}H NMR (DMSO-d_6, δ): 1.70 (dt, J = 5.6, 4.5 Hz, 2H, CH_2), 1.81 (dt, J = 8.9, 4.8 Hz, 2H, CH_2), 2.54 (t, J = 6.1 Hz, 2H, CH_2), 2.95 (t, J = 6.0 Hz, 2H, CH_2), 7.80 (t, J = 7.8 Hz, 1H, ArH), 7.94 (d, J = 7.7 Hz, 1H, ArH), 8.04 (dd, J = 5.4, 3.1 Hz, 2H, ArH), 8.13 (dd, J = 5.5, 3.0 Hz, 2H, ArH), 8.66 (s, 1H, ArH), 8.71 (d, J = 8.0 Hz, 1H, ArH); Analysis: Calc. for $C_{25}H_{16}F_3N_3O_2S$: C, 62.62; H, 3.36; F, 11.89; N, 8.76; O, 6.67; S, 6.69; Found: C, 62.62; H, 3.37; F, 11.89; N, 8.76; O, 6.66; S, 6.70; Method B: Yield: 65%.

2.1.5. Theoretical calculations

The quantum chemical calculations were performed using the Gaussian 09 package [32] of programs. Geometry optimization was carried out by analytical gradient technique without any symmetry constraint in gas phase. The results were obtained at DFT level of theory using B3LYP/6-311 + G** [33,34]. The stationary points found on the molecular potential energy hypersurfaces were characterized using standard harmonic vibrational analysis.

2.2. Evaluation of DNase I inhibition

Thieno[2,3-*d*]pyrimidine-4-amines **2**, **3**, **5**–**13** and their phthalimide derivatives **14**, **16**, **18**–**21** were investigated for the inhibitory effect towards bovine pancreatic DNase I. The *in vitro* evaluation of DNase I inhibition is based on spectrophotometric measurement of acid-soluble nucleotides formation at 260 nm according to the method previously described [10], using crystal violet as a positive control.

2.3. R-Group analysis

2.3.1. Pharma/E-State RQSAR models

Pharma/E-State RQSAR models, analyzed the thieno[2,3-*d*]pyrimidines activity as a function of the kind of R-group at each attachment position, and displayed the results qualitatively in terms of increasing, decreasing, or little effect on the activity [28]. We ran a partial-least-squares (PLS) procedure that fitted the observed inhibitory data to the counts of the features present in each R group at each position. For Pharma/E-State RQSAR models, the features counted are the pharmacophore types and various E-state atom types [28]. This was done using a 75%: 25% random training: test-set split. The procedure was repeated one hundred times, each time picking the model that does the best job without overfitting. For each model, each pharmacophore/E-state feature type at each R-group position was given a coefficient that reflects how much it contributes to the property being modeled. A feature type was deemed significant (colored red or blue) if the absolute value of the mean of its coefficients over the models exceeded the importance cutoff, which is a statistic computed from all coefficients over all models.

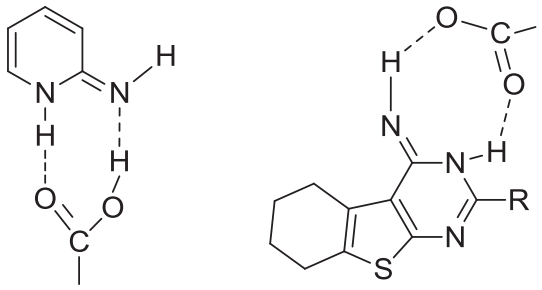

Fig. 2. The 2-aminopyridine and 2-substituted-4-amino-thieno[2,3-*d*]pyrimidines acetic acid complexes.

2.3.2. Importance analysis

Importance analysis addressed the question of how sensitive the DNase I inhibitory property of thieno[2,3-*d*]pyrimidines was to R group variation at specific position. A position was more important than another if varying the R group at that position led to greater property differences than are observed when the R group at the other position is varied. The importance value of a position was the range of the property over the R groups at specific position, averaged over all structures containing a given R group at that position.

2.4. Molecular docking

2.4.1. Ligand preparation

Examined thieno[2,3-*d*]pyrimidines were built with ChemBioDraw Ultra 13.0 (PerkinElmer, Inc.) and their geometries have been optimized with ChemBio 3D Ultra 13.0 (PerkinElmer, Inc.) using MM2

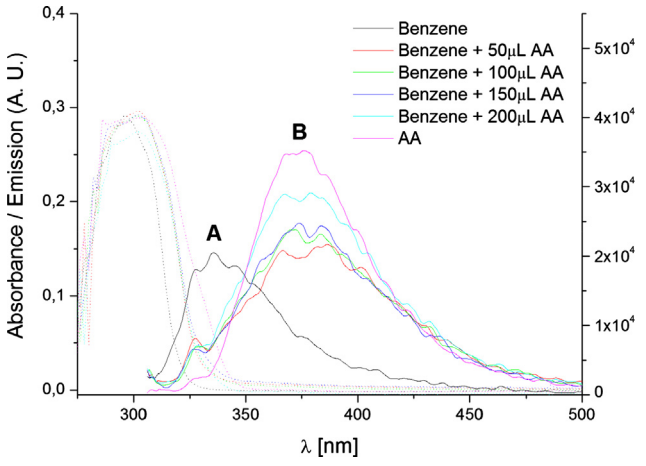

Fig. 3. Absorbance (dashed line) and emission (solid line) spectra of compound **3** in benzene with addition of acetic acid (AA).

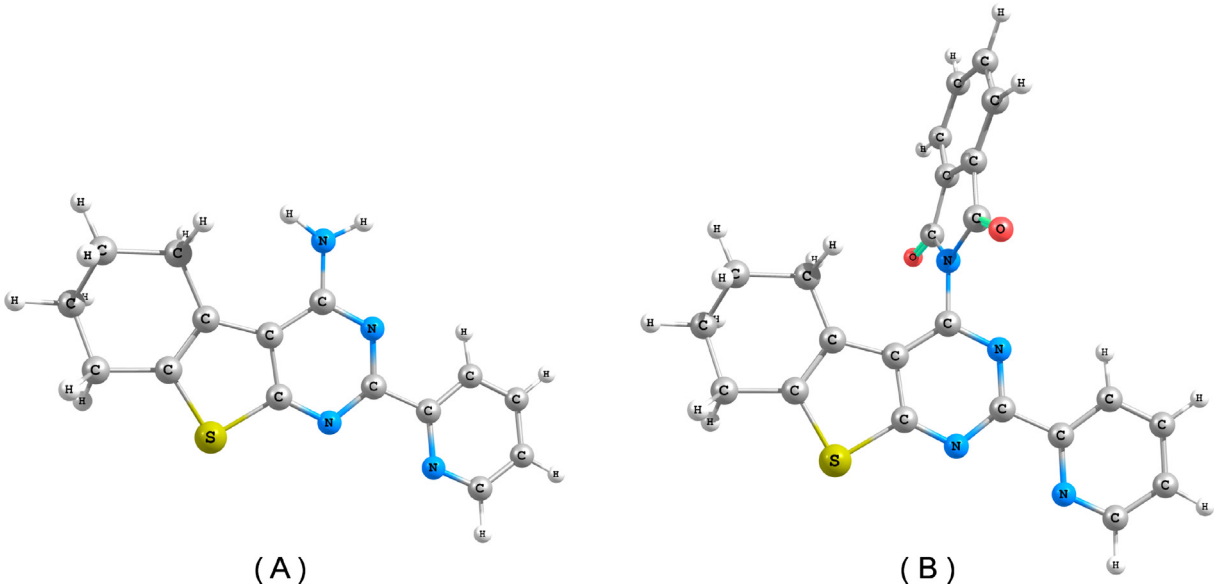

Fig. 4. DFT optimized structure of representative thieno[2,3-*d*]pyrimidine-4-amine **7** and its phthalimide derivative **16**.

Table 1
In vitro DNase I inhibitory activity of the studied thieno[2,3-*d*]pyrimidines.

Comp.	IC_{50} (μM) ± SD	Comp.	IC_{50} (μM) ± SD	Comp.	IC_{50} (μM) ± SD
2	197 ± 13	**9**	> 200	**16**	134 ± 15
3	> 200	**10**	195 ± 14	**18**	148 ± 19
5	> 200	**11**	128 ± 17	**19**	106 ± 16
6	> 200	**12**	> 200	**20**	> 200
7	156 ± 29	**13**	148 ± 27	**21**	> 200
8	> 200	**14**	> 200	Crystal violet	383 ± 49

force field until a minimum 0.100 Root Mean Square (RMS) gradient was reached. Subsequently all compounds structures were followed by energy minimization with MMFF94x force field in the Molecular Operating Environment (MOE) Software package 2014.0901 [35]. Conformational search for preparation of the ligands was carried out by MOE LowModelMD method which performs molecular dynamics perturbations along with low frequency vibrational modes with energy window 7 kcal/mol, and conformational limits of 1000.

2.4.2. Receptor preparation

The X-ray crystallographic structure of a complex between DNase I and the self-complementary octamer duplex $d(GGTATACC)_2$ (PDB code: 1DNK) was obtained from the Protein Data Bank [36]. The errors of the DNase I were corrected by the Structure Preparation process in MOE. After the correction, hydrogens were added and partial charges (Gasteiger methodology) were calculated. Energy minimization (AMBER12:EHT, RMS gradient: 0.100) was performed.

2.4.3. Docking protocol

The molecular docking study was performed using MOE to understand the ligand protein interactions in detail. The Site Finder module of the MOE was used to identify ligand-binding pocket within the optimized structure of DNase I. The default Triangle Matcher placement method was used for the induced fit docking. GBVI/WSA dG scoring function which estimates the free energy of binding of the ligand from a given pose was used to rank the final poses. Each ligand protein complex with lowest relative binding free energy (ΔG) was selected. A more negative score indicates that ligand is more likely to dock with the receptor and achieve more favorable interactions.

3. Results and discussion

3.1. Synthesis

The 2-aminothiophene precursor has been prepared via a multicomponent condensation between appropriate malononitrile, cyclohexanone, sulfur and diethyl amine in conditions represented in the literature by Gewald [29]. The formation of the pyrimidine ring was performed by passing a stream of dry HCl gas through a dry dioxane solution [31]. The phthalimide derivatives **14–21** were synthesized by reaction of amines **2–13** with phthalic anhydride under reflux.

It is known that 2-aminopyrimidines form a cyclic complex with acetic acid via hydrogen bonds (Fig. 2) [37]. This leads to tautomerism and proton transfer in an excited state, resulting in the molecule going into an imino-form [38,39]. It is known that complex formation is a temperature-dependent process [40], as with increasing temperature the quantity of the complex increases. At the same time, it has been reported that in a polar environment the rising of temperature (energy) leads to displacement of equilibrium to imino-tautomer [38,41,42].

Based on these facts and the results obtained, it can be concluded that the low reactivity of 4-amino-5,6,7,8-tetrahydrobenzothieno[2,3-*d*]pyrimidines is due to a complex formation and tautomerisation which obstruct the process of acylation at high temperature. It can be assumed that the low yield of imide compounds **14–21** is related to the fact that 4-amino-pyrimidine and 2-amino-pyridine derivatives exhibit double H-bond 1:1 complex formation with acetic acid [37,39].

Spectrophotometric analysis of the 4-aminothiopyrimidine **3** was performed to establish the possibility of tautomerization of the reagent in acetic acid (AA) medium. For the experiment, compound **3** was

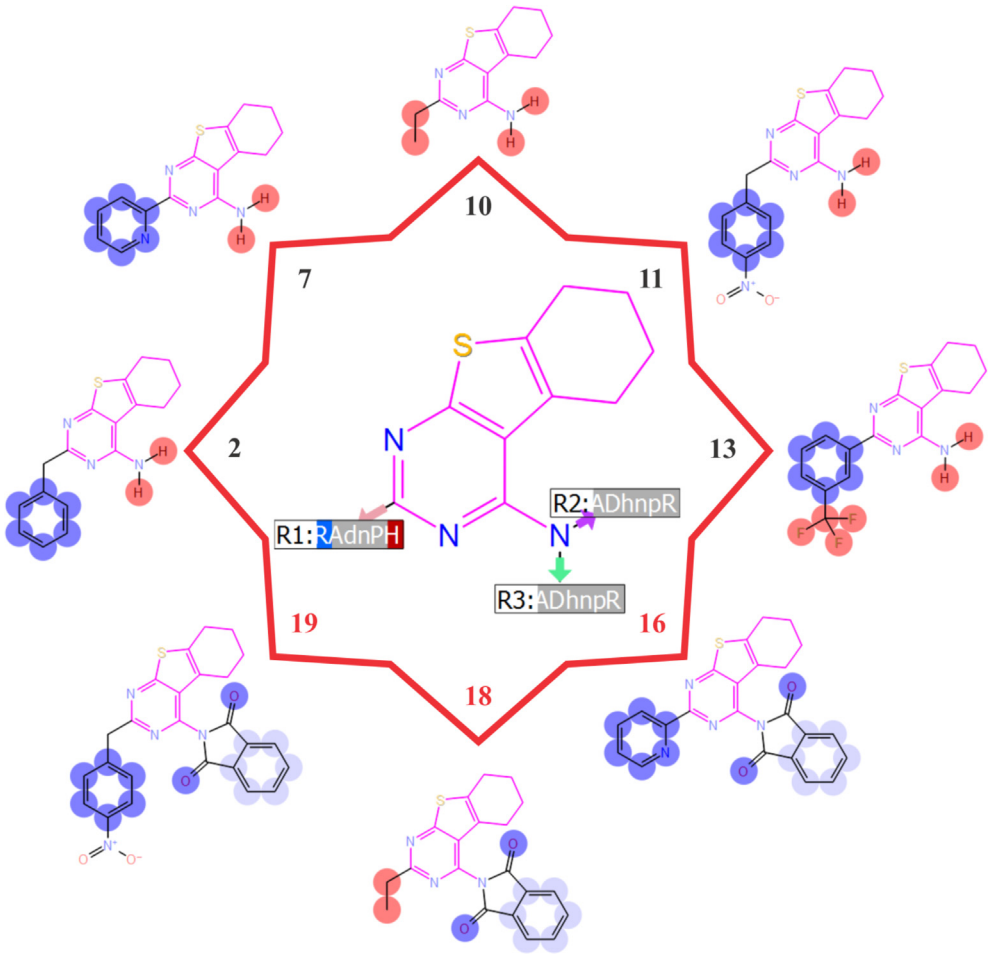

Fig. 5. The Pharma RQSAR model of the investigated series of thieno[2,3-*d*]pyrimidine-4-amines. The attachment positions on the thieno[2,3-*d*]pyrimidine scaffold were labeled with a list of pharmacophore features, colored by significance: blue for significant positive contributions, red for significant negative contributions, and gray for insignificant contributions to DNase I inhibition. If a pharmacophore feature was absent from an attachment position, a lower-case letter was used for the pharmacophore feature type. Examined pharmacophore features: hydrogen-bond acceptor (A), hydrogen-bond donor (D), hydrophobic (H), negatively-charged (N), positively-charged (P), and aromatic (R).

dissolved in non-polar solvents benzene ($\varepsilon = 2.3$). Fluorescence spectra were recorded at wavelength of excitation (λ_{ex}) corresponding to the absorption maximum of the compound in benzene.

It was observed (Fig. 3) that upon addition of AA to the analyte solution, the fluorescence band **A** corresponding to the analyte in a non-polar solvent was displaced batochromatically with large Stokes shift (**B**) and at the same time only insignificant batochromatic shift of absorbance of 6 nm was observed, which indicates the formation of a complex with the acetic acid. This result is in accordance with the spectroscopic evidences for acetic acid-2-iminopyridine complex formation previously reported [37–40].

Considering the above facts, we have set ourselves the aim to create a new approach for the synthesis of isoindoldiones in order to increase the yields and reduce the reaction time. The synthesis of isoindoldiones proceeded in good yields in one step if the interaction between the amine and phthalic anhydride was carried out by refluxing in toluene and without isolation of the formed intermediate acid. Acetic anhydride and pyridine were added and the reaction solution was refluxed 1–3 h more. After completion of the reaction, water was added, the aqueous solution was extracted with toluene and the organic layers were dried and concentrated under reduced pressure. This new approach results in the production of thienopyrimidine-isoindolones with significantly higher yields than the reaction in an acetic acid medium, and moreover the reaction time is repeatedly reduced.

Molecular structure optimization at DFT B3LYP/6-311 + + G** level of theory predicted planar structure of the thienopyrimidine moiety with approximately equal C-N distances in the ring. The structure of the thieno[2,3-*d*]pyrimidine-4-amines and their phthalimide derivatives is illustrated in Fig. 4 by compounds **7** and **16** bearing aryl substituent (2-pyridyl ring) at 2C position of the pyrimidine ring. Fig. S28 in the Supplementary material provides theoretically calculated bond lengths of the thienopyrimidine moiety for representative thieno[2,3-*d*]pyrimidine-4-amines and phthalimides within the studied series. The IR spectra of the thieno[2,3-*d*]pyrimidine-4-amines in solid state showed bands within the region 3350–3100 cm^{-1} confirming the presence of primary amino groups.

Based on the DFT optimization, the phthalimide fragment in the thienopyrimidine-isoindolones has almost perpendicular orientation (68–71°) in respect to the adjacent thienopyrimidine plane (Fig. 4B). The introduction of the phthalimide fragment leads to alteration of the bond lengths in the pyrimidine ring. On the other hand, the size and nature of the substituents attached at 5-position of the pyrimidine ring has little influence on the structural parameters of the phthalimide fragment (Fig. S28 Supplementary material). Accordingly, the IR spectra of all the thienopyrimidine-isoindolones displayed two characteristic bands for the stretching vibrations of phthalimide C═O groups varying in very narrow intervals – app. 1784 and 1722 cm^{-1}.

To the best of our knowledge, the synthesis of compounds **5**, **6**, **8**, **10**, **12–21** within this paper has been reported for the first time.

3.2. DNase I inhibition

Seventeen thieno[2,3-*d*]pyrimidines (**2**, **3**, **5–14**, **16** and **18–21**) were tested *in vitro* on inhibitory activity towards bovine pancreatic

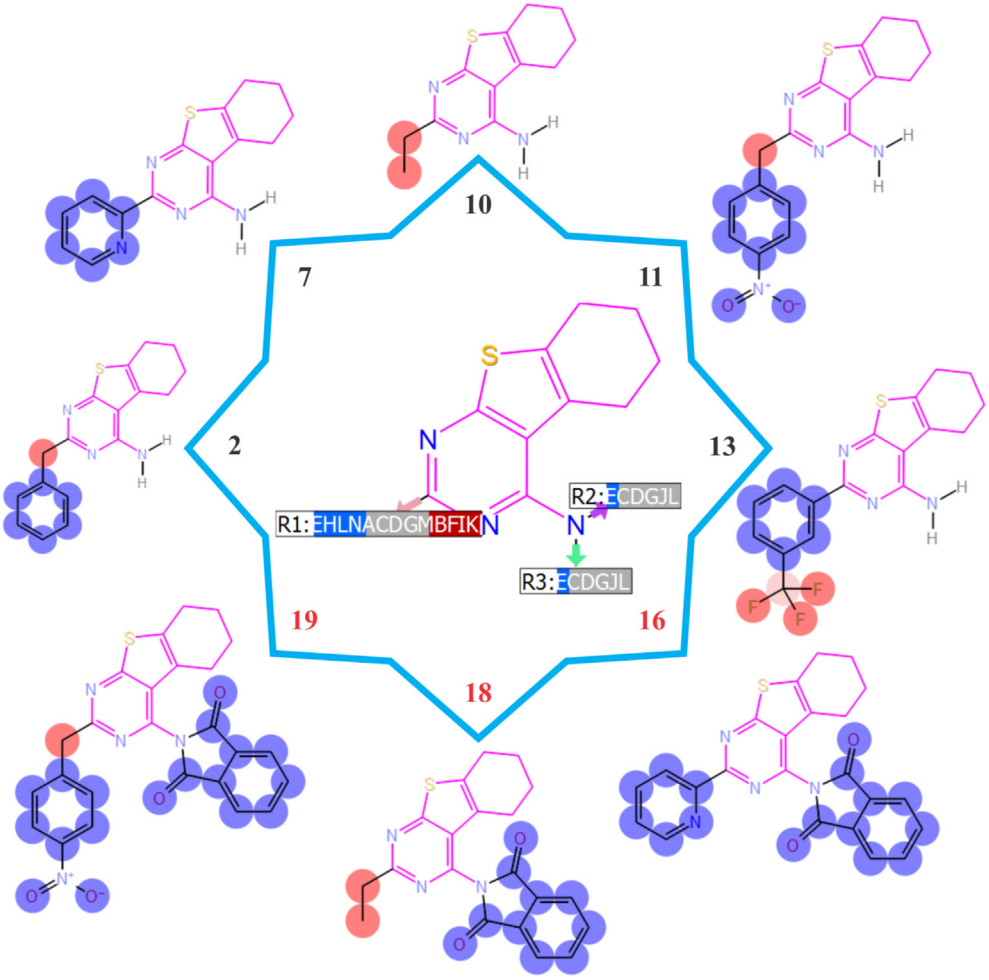

Fig. 6. The E-State RQSAR model of the investigated series of thieno[2,3-*d*]pyrimidine-4-amines. The attachment positions on the thieno[2,3-*d*]pyrimidine scaffold were labeled with a list of letters representing the E-state atom types (Table S2) colored by significance: blue for significant positive contributions, red for significant negative contributions, and gray for insignificant contributions to DNase I inhibition. If an E-state atom type was absent from an attachment position, it was not included in the annotation for that position.

DNase I. The obtained results were plotted and IC_{50} values were calculated (Table 1). Eight compounds, including five amino (**2**, **7**, **10**, **11** and **13**) and three phthalimide (**16**, **18** and **19**) derivatives, inhibited bovine pancreatic DNase I with IC_{50} values below 200 μM. Phthalimide derivative **19** and its amine precursor **11** showed the most potent inhibitory activity against DNase I, with IC_{50} values of 106 ± 16 and 128 ± 17 μM, respectively (Table 1). From a structural point of view, this affinity could be explained by the presence of *p*-NO_2 group in the side chain, which may contribute to better binding to the active enzyme center analogously to N═O derivatives. It can be noted that some of the phthalimide derivatives (**16**, **18** and **19**) exhibited higher inhibitory effect towards DNase I in comparison to the structurally related amino derivatives **7**, **10** and **11**. However, the examined phthalimides **14** and **21** showed lower DNase I inhibitory activity in respect to the thieno[2,3-*d*]pyrimidine-4-amines **2** and **13**. No difference in DNase I inhibition was observed between the two 3-chlorobenzoyl derivatives **12** and **20**. Crystal violet, a known organic DNase I inhibitor [43], was used as a standard and exhibited weaker inhibitory effect on commercial DNase I (IC_{50} = 383 ± 49 μM) compared to the studied compounds. Furthermore, the same thieno[2,3-*d*]pyrimidines exhibited a much higher DNase I inhibitory activity than natural DNase I inhibitor neomycin (completely inhibiting degradation of plasmid DNA *in vitro* at a concentration of 2 mM) [44] and synthetic DNase I inhibitor 2-nitro-5-thiocyanobenzoic acid (inhibiting DNase I with affinity constant of

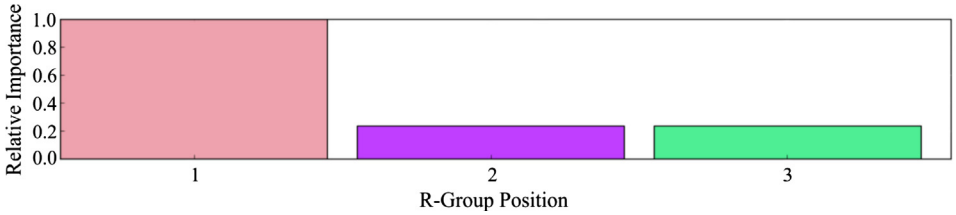

Fig. 7. The importance analysis histogram of the investigated series of thieno[2,3-*d*]pyrimidines.

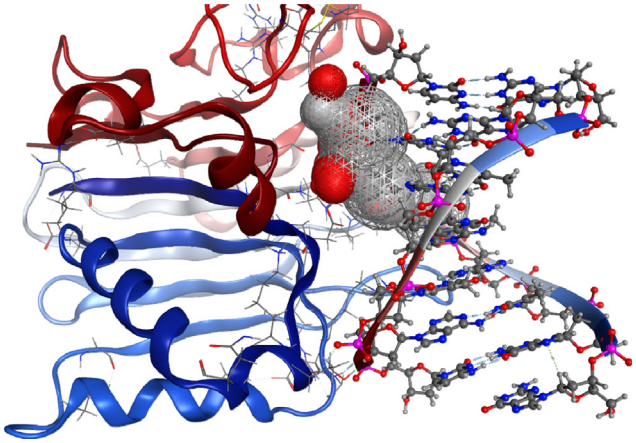

Fig. 8. The top ranked DNase I binding site, represented by a grey-red surface map.

approximately 16.7 mM) [45].

3.3. In silico studies

3.3.1. R-Group analysis

As Pharma RQSAR model showed, the presence of aryl substituents at R1 position of the studied thieno[2,3-*d*]pyrimidines have substantial increased DNase I inhibition (Table S1, Fig. 5). Furthermore, hydrogen-bond acceptor/donor substituents at all examined positions exerted an insignificant enhancement to the thieno[2,3-*d*]pyrimidines activity (Table S1). Additionally, the presence of hydrophobic substituents at R1 position resulted in a decreased DNase I inhibition (Table S1, Fig. 5). Next, we examined the effect of the E-State parameters of thieno[2,3-*d*]pyrimidines on the DNase I inhibition (Table S2, Fig. 6). As Table S2 shows, the introduction of aaCH, aaN, dO and sOm fragments at R1 position, as well as the introduction of aaCH fragment at R2 or R3 position, exerted a significant enhancement to the thieno[2,3-*d*]pyrimidines activity. On the contrary, the use of $ssCH_2$, sCH_3, ssO and sCl fragments at R1 position, resulted in a decreased DNase I inhibition (Table S2, Fig. 6). Additionally, we wanted to examine how sensitive DNase I inhibitory property of thieno[2,3-*d*]pyrimidines was to R group variation at specific position. As Fig. 7 shows, variation of substituents at R1 position had substantial effects on DNase I inhibition, compared to R2 or R3 position.

3.3.2. Molecular docking

The binding site residues in DNase I have been identified using the Site Finder module implemented in the MOE software [35]. The results from the analysis highlighted that amino acid residues like Asn 7, Arg 9, Glu 39, Tyr 76, Glu 78, Arg 111, His 134, Ala 136, Pro 137, Asp 168, Asn 170, Thr 203, Thr 205, Thr 207, Tyr 211, Asp 251 and His 252 constituted the binding pocket of the DNase I structure [10]. Our results are consistent with a recent study highlighting the conservation of the amino acids involved in the identified cation-binding sites across DNase I and DNase I-like protein [46]. It is worth mentioning that inhibitor-binding pocket, represented by a grey-red surface map, is within the region that interacts with DNA octamer $d(GGTATACC)_2$ (Fig. 8).

The intermolecular contacts between thieno[2,3-*d*]pyrimidines and DNase I were analyzed using the ligand interaction diagram of MOE suite. It illustrates the existence of hydrogen bond, pi-cation and H-pi interactions (Table S3). Additionally, the bond distances, bond energy and relative binding free energy between the inhibitor and receptor atoms were also examined. Of note, the importance of His 134 and His 252 residues in the catalytic mechanism of DNase I has been already highlighted [46]. It was confirmed that catalytic residues His 134 and His 252 are a part of the ion binding site IV, which is implicated in the cleavage of scissile phosphate. Furthermore, several site-directed mutagenesis experiments on the residues surrounding His 134 and His 252 demonstrated that single mutations on Glu 39 or Asp 168 residues, resulted in a very low activities on a DNA molecule [47]. The effects of these mutations also confirmed the active role of Glu 39 and Asp 168 in the IV catalytic site. In addition, as it was shown in the case of actin, steric effects may play a crucial role in DNase I inhibition [48].

The interaction profiles of thieno[2,3-*d*]pyrimidines with DNase I domain are shown in Figs. 9 and 10 and Table S3. Compound **11**, which corresponds to one of the most promising inhibitors in the non-phthalimide series, showed interactions with two catalytic histidines, His 134 and His 252. Furthermore, similar interactions with His 134 or His 252 were also observed for compounds **2**, **10** and **13** (Fig. 9, Table S3). Additionally, these compounds showed H-donor interactions with residues Glu 39 or Asp 168 (Table S3), which are also implicated in the cleavage of scissile phosphate [47]. The results from Table S3 indicate that thieno[2,3-*d*]pyrimidines **7**, **16**, **18** and **19**, were not found to possess any similar interactions as previously discussed compounds. Furthermore, these compounds showed generally increased DNase I inhibition compared to other thieno[2,3-*d*]pyrimidines (Table 1). Although interactions with catalytic residues are clearly important determinant of DNase I inhibitors [46,47], the results from Table 1 and Table S3 suggest that steric effects also play a vital role in DNase I inhibition [48]. For these reasons, the molecular size and flexibility of thieno[2,3-*d*]pyrimidines were calculated, and SAR analysis was accomplished. It was found that increase of molecular volume and weight leads to inhibitory enhancement (Fig. 11), and also confirms the importance of steric effects in DNase I inhibition (Table 1, Table S3).

3.3.3. SAR analysis

Noting that variations of the substituents at 2C position of the pyrimidine ring lead to slight changes in DNase I inhibition has drawn our attention to investigate the structure–activity relationship (SAR) of the amine and phthalimide derivatives that showed DNase I inhibition with IC_{50} below 200 μM. The mechanism of DNase I inhibition by crystal violet is based on its binding to the DNA matrix, thereby inhibiting its interaction with the enzyme [49]. Therefore, it is very important the studied thieno[2,3-*d*]pyrimidines to possess favourable pharmacokinetic properties, such as sufficient bioavailability and permeability through the different membranes to the desired receptor binding site, optimal metabolization and elimination profile. Thus, the calculated molecular properties, including lipophilicity, molecular size, flexibility and presence of hydrogen bond donors and acceptors could provide useful informations about SAR. According to the SAR analysis performed by Molinspiration tool [50], it could be seen that most of the compounds showing DNase I inhibition with IC_{50} below 200 μM are in accordance with Lipinski's "Rule of five" [51], having logP, MW, N_{HA} and N_{HD} values less than 5, 500, 10 and 5, respectively (Table 2). It appeared that compounds **13** and **19** are not in compliance with Lipinski's rule in regard of partition coefficient (logP), but possess relatively high DNase I inhibition activity. However, it has been reported that the lipophilicity of DNase I inhibitors is extended in a very broad range [52]. Moreover, all of the tested thienopyrimidine derivatives possess TPSA values lower than 140–150 $Å^2$ usually required for acceptable bioavailability (Table 2) [53]. Another important factor for the optimal bioavailability is moderate conformational flexibility which is described by the number of rotatable bonds (N_{rotb}) [54]. None of the compounds showing DNase I inhibition with IC_{50} below 200 μM has more than 10 rotatable bonds (Table 2) which is regarded as another sign of the expected good oral bioavailability.

It was found that the increase of molecular volume (Vol) leads to the enhancement of DNase I inhibition (Fig. 11A). The same effect was observed with the increase of sum of H-bond donor (N_{HD}) and H-bond acceptor (N_{HA}) groups multiplied with the molecular weight (MW) (Fig. 11B).

Considering toxicological properties calculated by DataWarrior

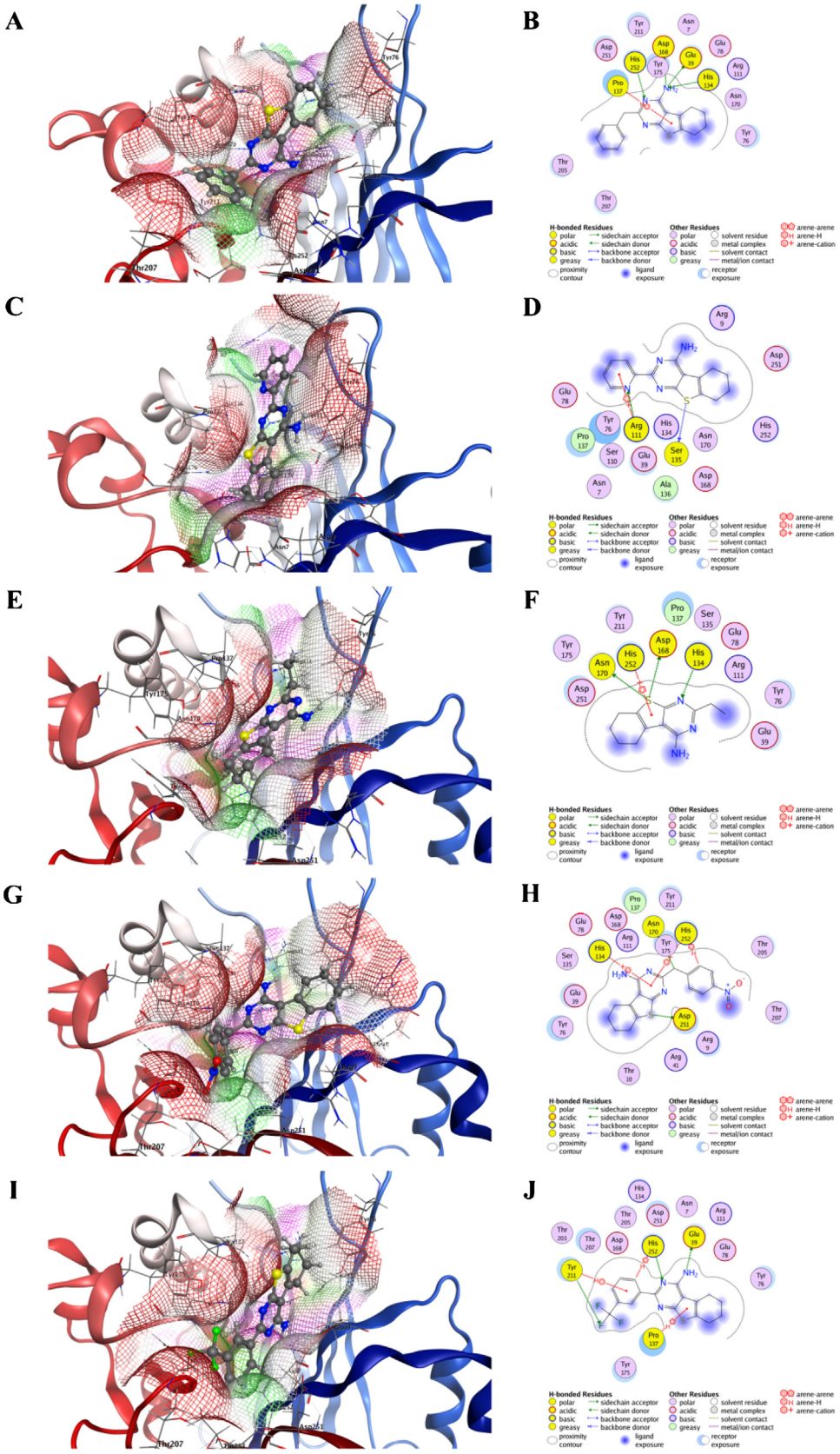

Fig. 9. 3D/2D view of compounds **2** (A, B), **7** (C, D), **10** (E, F), **11** (G, H) and **13** (I, J) bound in the active site of DNase I. The polar part of the active site is shown as a pink surface, hydrophobic part as a green surface, while the solvent exposed part is shown as a red surface.

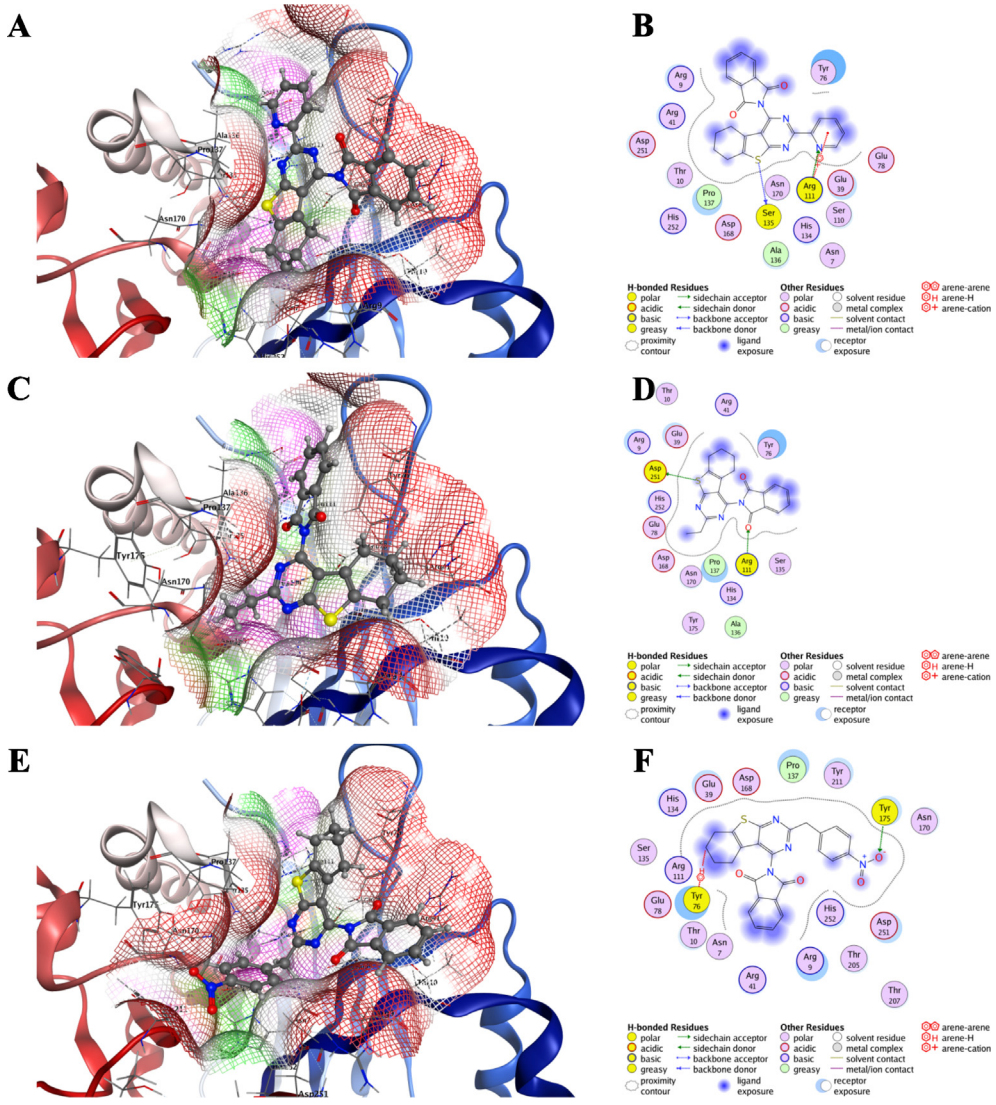

Fig. 10. 3D/2D view of compounds **16** (A, B), **18** (C, D) and **19** (E, F) bound in the active site of DNase I. The polar part of the active site is shown as a pink surface, hydrophobic part as a green surface, while the solvent exposed part is shown as a red surface.

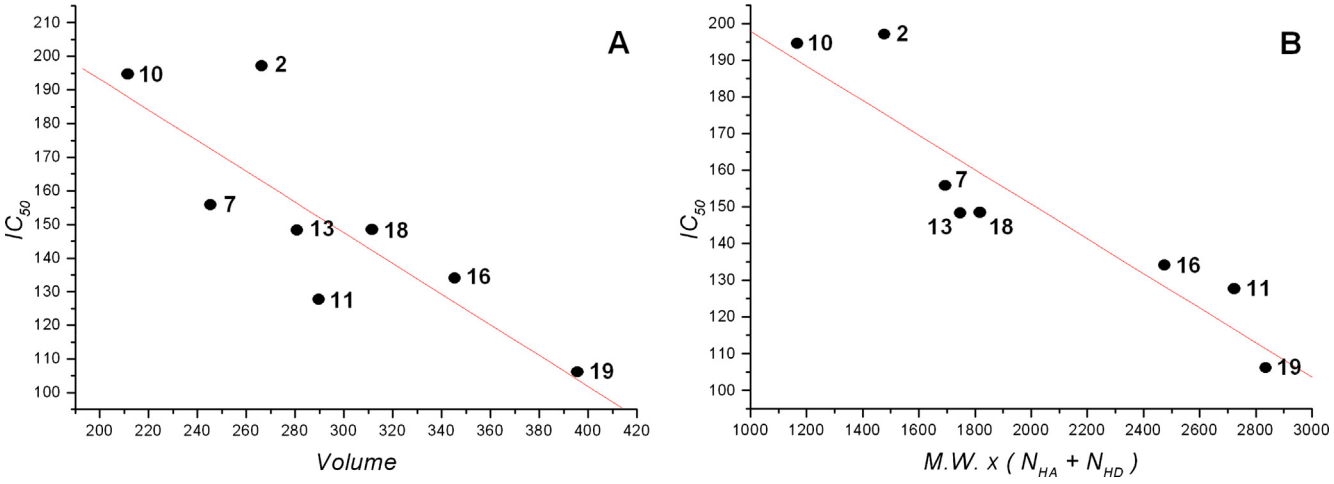

Fig. 11. SAR relationship of thieno[2,3-*d*]pyrimidines showing DNase I inhibition with IC_{50} below 200 μM.

Table 2
Calculated molecular properties of thieno[2,3-*d*]pyrimidines showing DNase I inhibition with IC_{50} below 200 μM.

Comp.	logP[a]	MW[b]	TPSA[c]	Vol[d]	N_{HA}[e]	N_{HD}[f]	N_{rotb}[g]
2	4.20	295.4	51.81	266.3	3	2	2
7	3.05	282.4	64.70	245.3	4	2	1
10	2.74	233.3	51.81	211.5	3	2	1
11	4.10	340.4	97.63	289.6	6	2	3
13	5.07	349.4	51.81	280.8	3	2	2
16	4.85	412.5	77.75	345.4	6	0	2
18	4.54	363.4	64.86	311.5	5	0	2
19	5.39	472.5	109.29	395.6	5	1	4

[a] Octanol-water partition coefficient, calculated by the methodology developed by Molinspiration.
[b] Molecular weight.
[c] Topologic polar surface area [$Å^2$].
[d] Molecular volume [$Å^3$].
[e] Number of hydrogen bond acceptors (O and N atoms).
[f] Number of hydrogen bond donors (OH and NH groups).
[g] Number of rotatable bonds.

[55], studied compounds were predicted as compounds with no mutagenic, tumorigenic, irritant risk, as well as compounds with no risk for reproductive effects.

4. Conclusion

A small library of twelve 2-substituted thieno[2,3-*d*]pyrimidin-4-amines were synthesized and used as precursors for preparation of eight new bipharmacophoric derivatives via cyclocondensation with phthalic anhydride. Evaluating DNase I inhibitory properties, eight of the amine and imide derivatives (**2**, **7**, **10**, **11**, **13**, **16**, **18** and **19**) inhibited bovine pancreatic DNase I activity *in vitro* with an IC_{50} below 200 μM and simultaneously exhibited higher inhibitory activity than crystal violet, used as positive control. Tested phthalimide derivatives **16**, **18** and **19** exhibited higher DNase I inhibition than their amine precursors **7**, **10** and **11**. The Pharma RQSAR model showed a significant enhancement of thieno[2,3-*d*]pyrimidines activity using aryl substituents at R1 position. The E-State RQSAR model clarified the most important structural fragments relevant for DNase I inhibition. Furthermore, the thieno[2,3-*d*]pyrimidines interactions with the most important catalytic residues of DNase I, including Glu 39, His 134, Asp 168 and His 252, were shown. It was found that steric effects and increase of molecular volume play a vital role in DNase I inhibition. These observations could be potentially utilized to guide the rational design and optimization of new thieno[2,3-*d*]pyrimidine inhibitors. As the most potent, compound **19** offers a good starting point for a design of new DNase I inhibitors.

Acknowledgements

The financial support of this work by Science Fund/Chemical Technology and Metallurgy University (Grant 11523), Ministry of Education, Science and Technological Development of the Republic of Serbia (Grants No. OI 172044, OI 171025 and TR 31060) and Faculty of Medicine of the University of Niš (Internal project No. 4) is gratefully acknowledged. The authors would like to thank Chemical Computing Group and Schrödinger LLC., for providing us the academic licenses free of cost for this study.

Conflict of interest

The authors declare that there are no conflicts of interest.

References

[1] D. Shiokawa, S.I. Tanuma, Characterization of human DNase I family endonucleases and activation of DNase γ during apoptosis, Biochemistry 40 (2001) 143–152.
[2] V. Kreuder, J. Dieckhoff, M. Sittig, H.G. Mannherz, Isolation, characterization and crystallization of deoxyribonuclease I from bovine and rat parotid gland and its interaction with rabbit skeletal muscle actin, Eur. J. Biochem. 139 (1984) 389–400.
[3] A. Funakoshi, H. Wakasugi, M. Nakamura, Y. Takagi, H. Ibayashi, Biochemical and clinical studies on human pancreatic deoxyribonuclease I inhibitor, Gastroenterol. Jpn. 15 (1980) 592–599.
[4] T. Yasuda, Y. Kawai, M. Ueki, K. Kishi, Clinical applications of DNase I, a genetic marker already used for forensic identification, Leg. Med. 7 (2005) 274–277.
[5] Y. Yamada, T. Fujii, R. Ishijima, H. Tachibana, N. Yokoue, R. Takasawa, S.I. Tanuma, DR396, an apoptotic DNase γ inhibitor, attenuates high mobility group box 1 release from apoptotic cells, Bioorg. Med. Chem. 19 (2011) 168–171.
[6] M.C. Peitsch, B. Polzar, H. Stephan, T. Crompton, H.R. MacDonald, H.G. Mannherz, J. Tschopp, Characterization of the endogenous deoxyribonuclease involved in nuclear DNA degradation during apoptosis (programmed cell death), EMBO J. 12 (1993) 371–377.
[7] F. Rauch, B. Polzar, H. Stephan, S. Zanotti, R. Paddenberg, H.G. Mannherz, Androgen ablation leads to an upregulation and intranuclear accumulation of deoxyribonuclease I in rat prostate epithelial cells paralleling their apoptotic elimination, J. Cell Biol. 137 (1997) 909–923.
[8] M. Oliveri, A. Daga, C. Cantoni, C. Lunardi, R. Millo, A. Puccetti, DNase I mediates internucleosomal DNA degradation in human cells undergoing drug-induced apoptosis, Eur. J. Immunol. 31 (2001) 743–751.
[9] S. Elmore, Apoptosis: a review of programmed cell death, Toxicol. Pathol. 35 (2007) 495–516.
[10] B.S. Ilić, A. Kolarević, G. Kocić, A. Šmelcerović, Ascorbic acid as DNase I inhibitor in prevention of male infertility, Biochem. Biophys. Res. Commun. 498 (2018) 1073–1077.
[11] N.G. Haswani, S.B. Bari, Synthesis and antimicrobial activity of novel 2-(pyridin-2-yl)thieno[2,3-*d*]pyrimidin-4 (3*H*)-ones, Turk. J. Chem. 35 (2011) 915–924.
[12] W.A. El-Sayed, O.M. Ali, R. Zyada, A.A. Mohamed, A.A. Abdel-Rahman, Synthesis and antimicrobial activity of new substituted thienopyrimidines, their tetrazolyl and sugar derivatives, Acta Pol. Pharm. 69 (2011) 439–447.
[13] A. Cohen, P. Suzanne, J.C. Lancelot, P. Verhaeghe, A. Lesnard, L. Basmaciyan, S. Hutter, M. Laget, A. Dumètre, L. Paloque, E. Deharo, M.D. Crozet, P. Rathelot, P. Dallemagne, A. Lorthiois, C.H. Sibley, P. Vanelle, A. Valentin, D. Mazier, S. Rault, N. Azas, Discovery of new thienopyrimidinone derivatives displaying antimalarial properties toward both erythrocytic and hepatic stages of *Plasmodium*, Eur. J. Med. Chem. 95 (2015) 16–28.
[14] H.M. Ashour, O.G. Shaaban, O.H. Rizk, I.M. El-Ashmawy, Synthesis and biological evaluation of thieno[2',3':4,5]pyrimido[1,2-b][1,2,4]triazines and thieno[2,3-d][1,2,4]trizolo[1,5-a]pyrimidines as anti-inflammatory and analgesic agents, Eur. J. Med. Chem. 62 (2013) 341–351.
[15] H.N. Hafez, O.K. Al-Duaij, A.R.B.A. El-Gazzar, Design, synthesis and pharmacological evaluation of new nonsteroidal anti-inflammatory derived from 3-aminobenzothieno[2,3-*d*]pyrimidines, Int. J. Org. Chem. 3 (2013) 110–118.
[16] S. Pédeboscq, D. Gravier, F. Casadebaig, G. Hou, A. Gissot, C. Rey, F. Ichas, F. De Giorgi, L. Lartigue, J.P. Pometan, Synthesis and evaluation of apoptosis induction of thienopyrimidine compounds on KRAS and BRAF mutated colorectal cancer cell lines, Bioorg. Med. Chem. 20 (2012) 6724–6731.
[17] Y. Kotaiah, N. Harikrishna, K. Nagaraju, C.V. Rao, Synthesis and antioxidant activity of 1,3,4-oxadiazole tagged thieno[2,3-*d*]pyrimidine derivatives, Eur. J. Med. Chem. 58 (2012) 340–345.
[18] M. Modica, G. Romeo, L. Materia, F. Russo, A. Cagnotto, T. Mennini, R. Gáspár, G. Falkay, F. Fülöp, Synthesis and binding properties of novel selective 5-HT_3 receptor ligands, Bioorg. Med. Chem. 12 (2004) 3891–3901.
[19] M.A. El-Sherbeny, M.B. El-Ashmawy, H.I. El-Subbagh, A.A. El-Emam, F.A. Badria, Synthesis, antimicrobial and antiviral evaluation of certain thienopyrimidine derivatives, Eur. J. Med. Chem. 30 (1995) 445–449.
[20] N.L. Shirole, K.D. Shirole, R.D. Deore, R.A. Fursule, G.S. Talele, Synthesis, characterization and pharmacological evaluation of 2-substituted thieno[2,3-d]pyrimidine-4(3H)-ones, Asian J. Chem. 19 (2007) 4985–4992.
[21] V. Alagarsamy, S. Meena, K.V. Ramseshu, V.R. Solomon, K. Thirumurugan, K. Dhanabal, M. Murugan, Synthesis, analgesic, anti-inflammatory, ulcerogenic index and antibacterial activities of novel 2-methylthio-3-substituted-5,6,7,8-tetrahydrobenzo (*b*) thieno[2,3-*d*]pyrimidin-4(3*H*)-ones, Eur. J. Med. Chem. 41 (2006) 1293–1300.
[22] V. Alagarsamy, S. Vijayakumar, V.R. Solomon, Synthesis of 2-mercapto-3-substituted-5,6-dimethylthieno[2,3-*d*]pyrimidin-4(3*H*)-ones as new analgesic, anti-inflammatory agents, Biomed. Pharmacother. 61 (2007) 285–291.
[23] J.L. Santos, P.R. Yamasaki, C.M. Chin, C.H. Takashi, F.R. Pavan, C.Q.F. Leite, Synthesis and in vitro anti *Mycobacterium tuberculosis* activity of a series of phthalimide derivatives, Bioorg. Med. Chem. 17 (2009) 3795–3799.
[24] M.A. Bhat, M.A. Al-Omar, Synthesis, characterization and *in vivo* anticonvulsant and neurotoxicity screening of Schiff bases of phthalimide, Acta Pol. Pharm. 68 (2011) 375–380.
[25] V. Bailleux, L. Vallee, J.P. Nuyts, J. Vamecq, Synthesis and anticonvulsant activity of some N-phenylphthalimides, Chem. Pharm. Bull. 42 (1994) 1817–1821.
[26] R.A. Pophale, M.N. Deodhar, Synthesis and evaluation of novel phthalimide derivatives as analgesic and anti-inflammatory agents, Der. Pharma Chem. 2 (2010) 185–193.
[27] W. Pluempanupat, S. Adisakwattana, S. Yibchok-Anun, W. Chavasiri, Synthesis of *N*-phenylphthalimide derivatives as α-glucosidase inhibitors, Arch. Pharm. Res. 30 (2007) 1501–1506.
[28] Small-Molecule Drug Discovery Suite 2015-1, Schrödinger, LLC, New York, NY, 2015.

[29] K. Gewald, E. Schinke, H. Böttcher, Heterocyclen aus CH-aciden Nitrilen, VIII. 2-Amino-thiophene aus methylenaktiven Nitrilen, Carbonylverbindungen und Schwefel, Chem. Ber. 99 (1966) 94–100.
[30] R.W. Sabnis, D.W. Rangnekar, N.D. Sonawane, 2-Aminothiophenes by the Gewald reaction, J. Heterocycl. Chem. 36 (1999) 333–345.
[31] C.J. Shishoo, M.B. Devani, V.S. Bhadti, K.S. Jain, S. Ananthan, Reaction of nitriles under acidic conditions. Part VI. Synthesis of condensed 4-chloro- and 4-amino-pyrimidines from *ortho*-aminonitriles, J. Heterocycl. Chem. 27 (1990) 119–126.
[32] M.J. Frisch, G.W. Trucks, H.B. Schlegel, G.E. Scuseria, M.A. Robb, J.R. Cheeseman, G. Scalmani, V. Barone, B. Mennucci, G.A. Petersson, H. Nakatsuji, M. Caricato, X. Li, H.P. Hratchian, A.F. Izmaylov, J. Bloino, G. Zheng, J. Sonnenberg, M. Hada, M. Ehara, K. Toyota, R. Fukuda, J. Hasegawa, M. Ishida, T. Nakajima, Y. Honda, O. Kitao, H. Nakai, T. Vreven, D.A. Montgomery, J.E. Peralta, F. Ogliaro, M. Bearpark, J.J. Heyd, E. Brothers, K.N. Kudin, V.N. Staroverov, R. Kobayashi, J. Normand, K. Raghavachari, A. Rendell, J.C. Burant, S. Iyengar, J. Tomasi, M. Cossi, N. Rega, J.M. Millam, M. Klene, J. Knox, J.B. Cross, V. Bakken, C. Adamo, J. Jaramillo, R. Gomperts, R. Stratmann, O. Yazyev, A.J. Austin, R. Cammi, C. Pomelli, J.W. Ochterski, R.L. Martin, K. Morokuma, V.G. Zakrzewski, G.A. Voth, P. Salvador, J.J. Dannenberg, S. Dapprich, A. Daniels, O. Farkas, J.B. Foresman, J.V. Ortiz, J. Cioslowski, D.J. Fox, Gaussian 09, Revision A1, Gaussian Inc., Wallingford CT, 2009.
[33] A.D. Becke, Density functional thermochemistry. III. The role of exact exchange, J. Chem. Phys. 98 (1993) 5648–5652.
[34] C. Lee, W. Yang, G.R. Parr, Development of the Colle-Salvetti correlation-energy formula into a functional of the electron density, Phys. Rev. B. 37 (1988) 785–789.
[35] Molecular Operating Environment (MOE) 2014.0901; Chemical Computing Group Inc., 1010 Sherbooke St. West, Suite #910, Montreal, QC, Canada, H3A 2R7, 2014.
[36] S.A. Weston, A. Lahm, D. Suck, X-ray structure of the DNase I-d(GGTATACC)$_2$ complex at 2.3 Å resolution, J. Mol. Biol. 226 (1992) 1237–1256.
[37] K. Inuzuka, A. Fujimoto, The amino–imino tautomerization of the 2-aminopyridine–acetic acid system in isooctane, Bull. Chem. Soc. Jpn. 63 (1990) 971–975.
[38] F.T. Hung, W.P. Hu, T.H. Li, C.C. Cheng, P.T. Chou, Ground and excited-state acetic acid catalyzed double proton transfer in 2-aminopyridine, J. Phys. Chem. A. 107 (2003) 3244–3253.
[39] A. Fujimoto, K. Inuzuka, Absorption and fluorescence spectra of 1-methyl-2(1*H*)-pyridinimines and 2-methylaminopyridine–acetic acid complex, Bull. Chem. Soc. Jpn. 64 (1991) 3758–3760.
[40] K. Inuzuka, A. Fujimoto, Electronic properties and ultraviolet absorption and fluorescence spectra of 2-pyridinamine, Spectrochim. Acta A. 42 (1986) 929–937.
[41] S. Chai, G.J. Zhao, P. Song, S.Q. Yang, J.Y. Liu, K.L. Han, Reconsideration of the excited-state double proton transfer (ESDPT) in 2-aminopyridine/acid systems: role of the intermolecular hydrogen bonding in excited states, Phys. Chem. Chem. Phys. 11 (2009) 4385–4390.
[42] D. Shugar, B. Kierdaszuk, New light on tautomerism of purines and pyrimidines and its biological and genetic implications, J. Biosci. 8 (1985) 657–668.
[43] Z. Zhou, C. Zhu, J. Ren, S. Dong, A graphene-based real-time fluorescent assay of deoxyribonuclease I activity and inhibition, Anal. Chim. Acta. 740 (2012) 88–92.
[44] M. Woegerbauer, H. Burgmann, J. Davies, W. Graninger, DNase I induced DNA degradation is inhibited by neomycin, J. Antibiot. 53 (2000) 276–285.
[45] T.H. Liao, L.J. McKenzie, Inactivation of bovine pancreatic DNase by 2-nitro-5-thiocyanobenzoic acid. I. A novel inhibitor for DNase I, J Biol. Chem. 254 (1979) 9598–9601.
[46] M. Guéroult, D. Picot, J. Abi-Ghanem, B. Hartmann, M. Baaden, How cations can assist DNase I in DNA binding and hydrolysis, PLoS Comput. Biol. 6 (2010) e1001000.
[47] S.J. Jones, A.F. Worrall, B.A. Connolly, Site-directed mutagenesis of the catalytic residues of bovine pancreatic deoxyribonuclease I, J. Mol. Biol. 264 (1996) 1154–1163.
[48] J.S. Ulmer, A. Herzka, K.J. Toy, D.L. Baker, A.H. Dodge, D. Sinicropi, S. Shak, R.A. Lazarus, Engineering actin-resistant human DNase I for treatment of cystic fibrosis, Proc. Natl. Acad. Sci. USA 93 (1996) 8225–8229.
[49] J.E. Cleaver, Repair replication of mammalian cell DNA: effects of compounds that inhibit DNA synthesis or dark repair, Radiat. Res. 37 (1969) 334–348.
[50] Molinspiration Cheminformatics, Molinspiration property engine v2015.01; http://www.molinspiration.com: 2015.
[51] C.A. Lipinski, F. Lombardo, B.W. Dominy, P.J. Feeney, Experimental and computational approaches to estimate solubility and permeability in drug discovery and development settings, Adv. Drug. Deliv. Rev. 46 (2001) 3–26.
[52] A. Kolarevic, D. Yancheva, G. Kocic, A. Smelcerovic, Deoxyribonuclease inhibitors, Eur. J. Med. Chem. 88 (2014) 101–111.
[53] H. Kubinyi, G. Folkers, R. Mannhold, Molecular drug properties: measurement and prediction, John Wiley & Sons: Weinhelm, 2008.
[54] D.F. Veber, S.R. Johnson, H.Y. Cheng, B.R. Smith, K.W. Ward, K.D. Kopple, Molecular properties that influence the oral bioavailability of drug candidates, J. Med. Chem. 45 (2002) 2615–2623.
[55] DataWarrior (http://www.openmolecules.org/datawarrior/).